Science and Technology Publishing (SCI & TECH)
ISSN: 2632-1017
Vol. 4 Issue 9, September - 2020

Device Hardware Capacity And Rssi-Based Self Organizing Map Clustering Of 928 Mhz Lorawan Nodes Located In Flat Terrain With Light Tree Densities

Ogbonna Chima Otumdi[1]
Department of Electrical/Electronic and Computer Engineering
University of Uyo
samwalliuy@yahoo.com

Ozuomba, Simeon[2]
Department of Electrical/Electronic and Computer Engineering
University of Uyo
simeonoz@yahoomail.com
simeonozuomba@uniuyo.edu.ng

Philip M. Asuquo[3]
Department of Electrical/Electronic and Computer Engineering
University of Uyo

***Abstract*— In this paper, device hardware capacity and received signal strength intensity (RSSI)-based self organizing map (SOM) clustering of 928 MHz Long Range Wide Area Network (LORAWAN) nodes located in flat terrain with light tree densities is presented. The case study was LORAWAN with 100 nodes distributed randomly over a 1200 m by 1200 m area. The RSSI was determined based on Erceg pathloss model employed in link budget formula. The hardware capacity range for the sensor nodes is such that 0 ≤ hardware capacity ≤ 5 whereas the hardware capacity range for the cluster sensor nodes is such that hardware capacity > 4.0. The RSSI range for the selecting the cluster head from the sensor nodes is such that -60 dB ≤ RSSI ≤ -75 dB. The result of the SOM clustering shows that 16 cluster heads were selected from the 100 sensor nodes. Also, the 16th cluster head with RSSI of -63 dB and hardware capacity of 4.564 had the highest number of 9 slave sensor nodes whereas , the 2nd cluster head with RSSI of -70.066dB and hardware capacity of 4.8496 and 3rd cluster heads with RSSI of -70.254dB and hardware capacity of 4.9843 had the lowest number of 3 slave sensor nodes.**

***Keywords*— LORAWAN , Clustering , Hardware Capacity, Received Signal Strength Intensity, Self Organizing Map, Sensor Nodes**

I. INTRODUCTION

Since the emergence of smart city concept [1,2,3], efforts have been on the increase to develop networks that are suitably adapted for smart city applications. Among others, Long Range Wide Area Network (LORAWAN) has been developed for such purpose [4,5,6,7,8,9,10]. The LORAWAN operates in different frequencies but in the North America the LORAWAN operates from 902-928MHz [11,12,13,14,15].

Apart from network type, energy efficiency is another issue that is highly desired in wireless sensor networks (WSN) [16,17,18,19,20]. In this wise, clustering of WSN nodes for device-to-device application is one of the popular approaches that is employed to minimize the overall transmission energy demand in a WSN [21,22,23,24]. Accordingly, in his paper, the study on the clustering of WSN nodes using self organizing map (SOM) clustering algorithm [26,27,28,29,30] is presented.

Furthermore, studies have shown that atmospheric condition of the propagation path, the terrain parameters and environmental parameter do affect the RSSI in WSN [31,32,33,34,35]. As such, the study focuses on the LORAWAN WSN located in flat terrain with light tree densities as defined in the Erceg pathloss model [36,37,38,39]. This is because, the environmental factors significantly affect the propagation loss and hence the RSSI in WSN.

Again, the SOM algorithm utilized the RSSI and the WSN nodes hardware capacity for the selection of the cluster heads. The whole computations and the SOM clustering implementations are conducted using Matlab software.

II. METHODOLOGY

2.1 DETERMINATION OF THE RECEIVE SIGNAL STRENGTH

The study is about the selection of cluster heads from among the network nodes in a LORAWAN network. The selection is based on the device hardware capacity and the received signal strength intensity (RSSI). The RSSI in dB (denoted as RSS(dB)) is determined using Erceg pathloss model employed in the link budget formula, as follows;

$$\text{RSSI(dB)} = \text{EIRP} - PL_{Erceg}\,(\text{dB}) \quad (1)$$

Where EIRP = effective isotropic radiated power in dB and PL_{Erceg} (dB) = pathloss in dB baed on Erceg pathloss model. Now, pathloss by Erceg model for flat terrain with light tree densities is given as [36,37,38,39].

$$PL_{Erceg}\,(\text{dB}) = A + 10\gamma\left(\log_{10}\left(\frac{d}{100}\right)\right) + X_f + X_h + S\ for\ d > 100 \quad (2)$$

Where,

f is frequency in MHz and X_f is frequency correction factor in MHz

S is the shadowing correction parameter in dB and 8.2 dB $\leq S \leq$ 10.6 dB

d is path length in km

Also,

$$A = 20\left(\log_{10}\left(\frac{400\pi}{\lambda}\right)\right) \quad (3)$$

γ is path loss exponent, where;

$$\gamma = 3.6 + 0.005(h_b) + \frac{20}{h_b} \quad (4)$$

The parameter h_b is the base station antenna height in meters and 10 m $\leq h_b \leq$80 m. The frequency correction factor Xf is given as:

$$X_f = 6\left(\log_{10}\left(\frac{f}{2000}\right)\right) \quad (5)$$

X_h is receiving antenna height correction factor in meters and it is given as;

$$X_h = -20.8\left(\log_{10}\left(\frac{h_m}{2}\right)\right) \quad (6)$$

Where, f is the frequency in MHz, and h_m is the receiver antenna height in meter.

2.2 THE HARDWARE CAPACITY AND PATH LENGTH DATA

In the LORAWAN network, 100 sensor nodes (devices) are considered. The hardware capacity of each of the 100 nodes is generated using Matlab function for random number (in Figure 1), where the range of values uses is $0 \leq$ hardware capacity $\leq$ 5. The RSSI range for the cluster sensor nodes is such that -60 dB $\leq$ RSSI $\leq$ -75 dB.

Also, the 100 sensor devices are randomly located in a network coverage area of 1200 m by 1200 m where the LORAWAN gateway (or base station) is located at the center of the LORAWAN network (that is , at coordinate of 600 m by 600 m) , as shown in Figure 2. Pythagoras formula was used to compute the distance of each of the sensor devices from the LORAWAN gateway. Then, the distance was used in the Erceg pathloss formula (Eq 2) to compute the pathloss which was in turn used in the link budget formula (Eq 1) to compute the RSSI . The scatter plot of the distance (m) of the sensor devices from the LORAWAN Gateway is shown in Figure 3. The scatter plot of computed pathloss and RSSI are shown in Figure 4 and Figure 4. The numerical values obtained for the 100 sensor devices x and y coordinates, distance, RSSI, hardware capacity are given in Table 1.

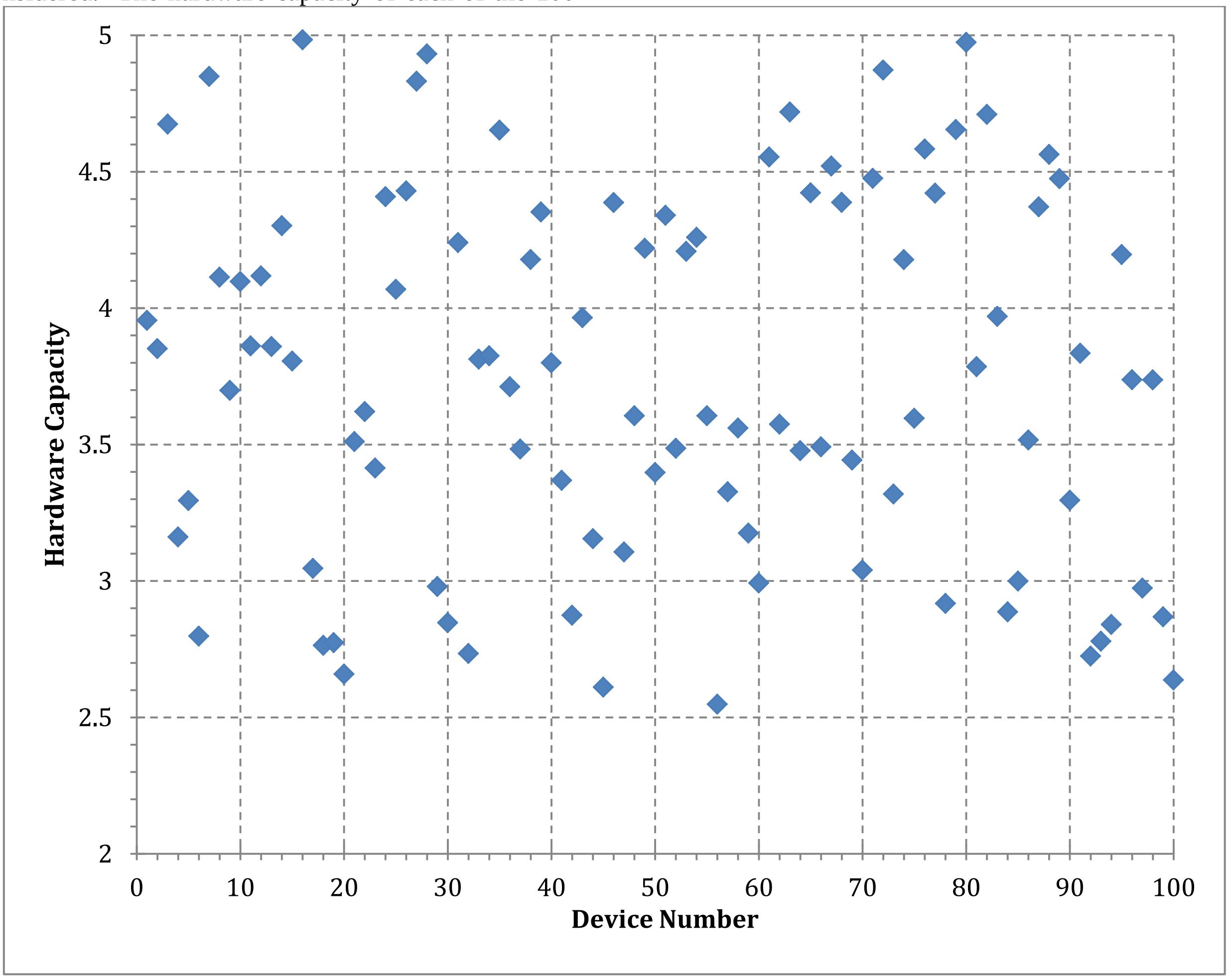

Figure 1 The hardware capacity of each of the 100 sensor nodes

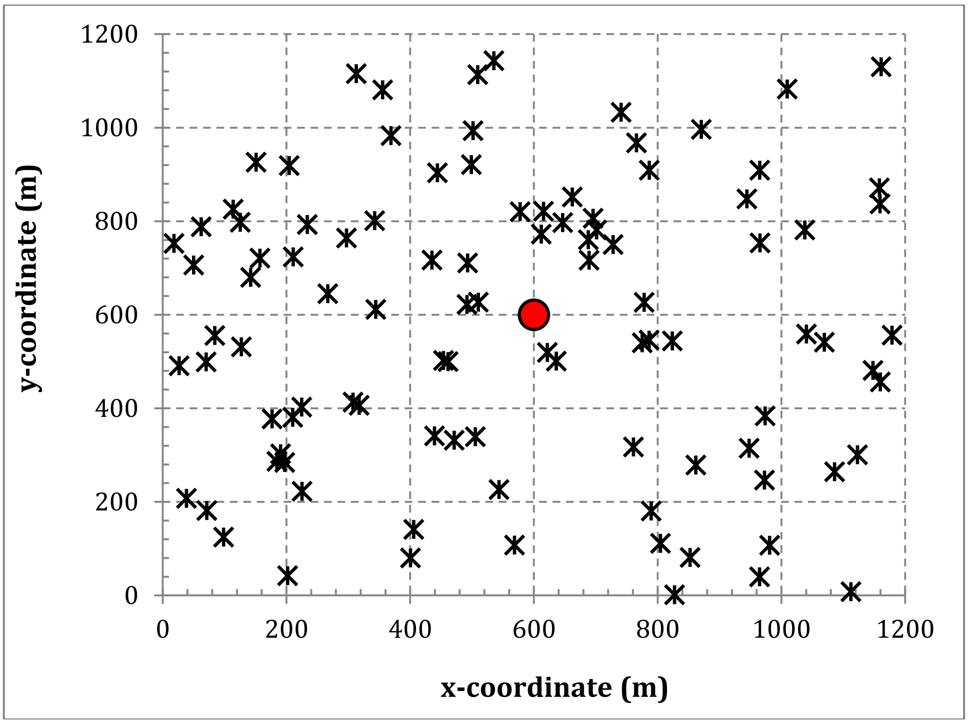

Figure 2; The x and y coordinate positions of the sensor devices.

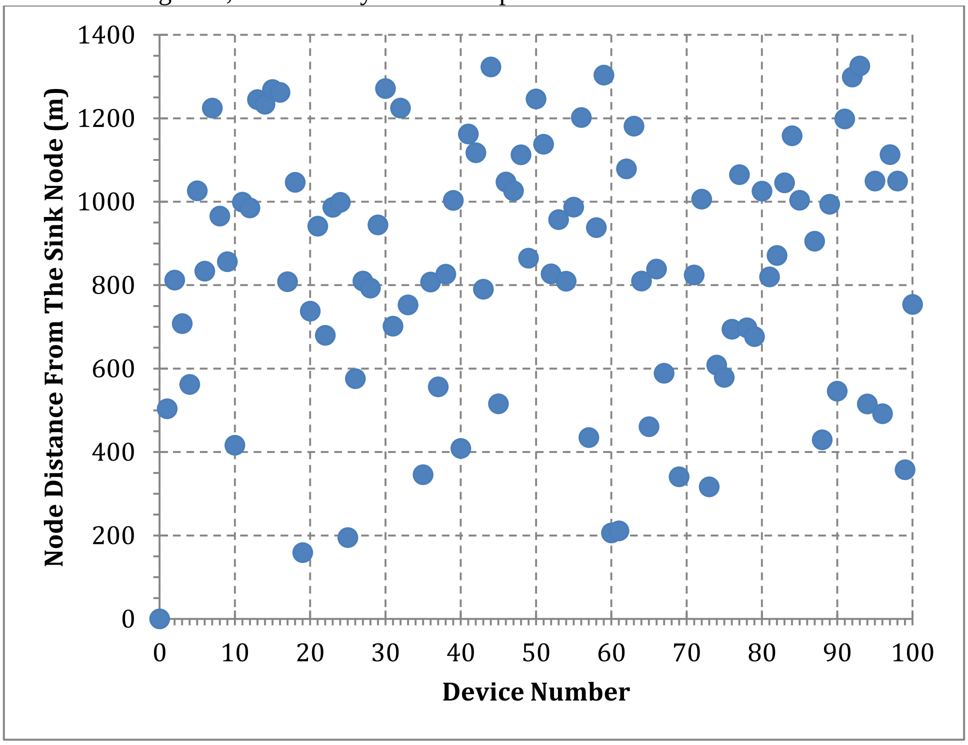

Figure 3; The scatter plot of the distance (m) of the sensor devices from the LORAWAN Gateway

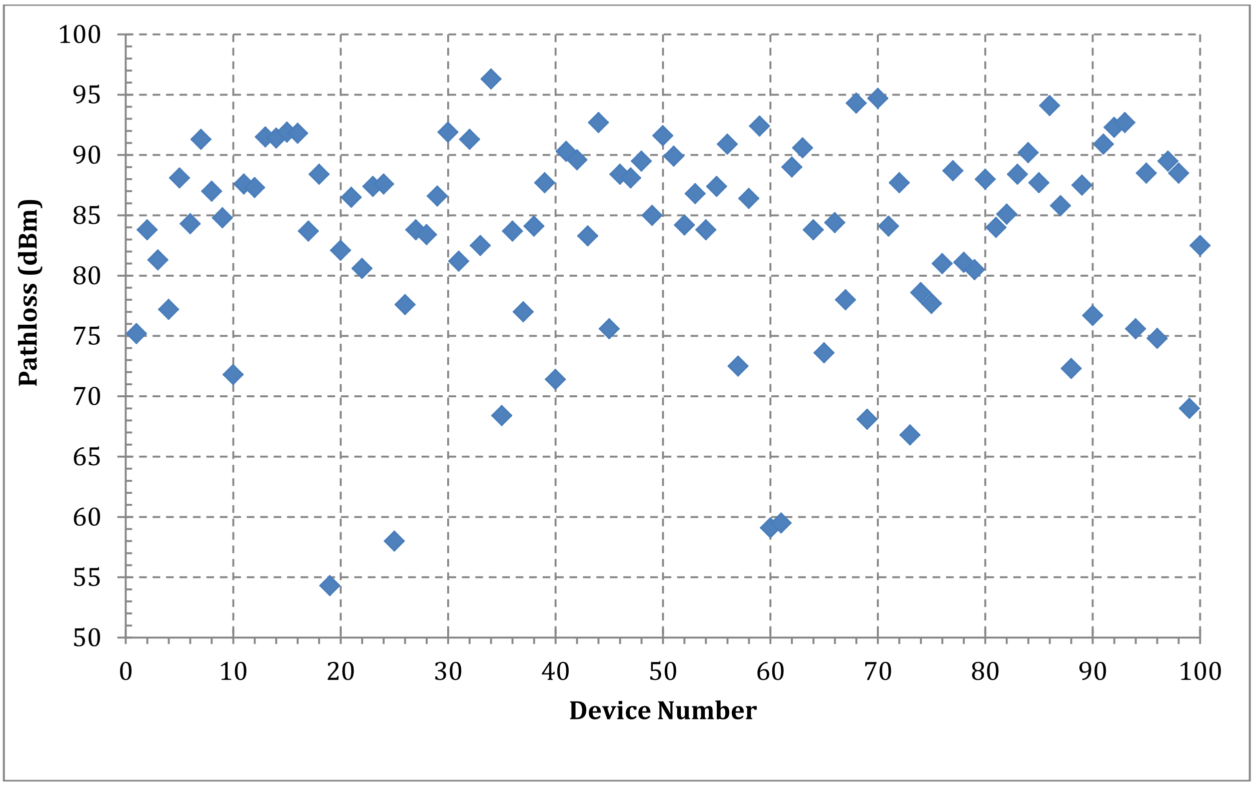

Figure 4; The scatter plot of the computed pathloss of each device.

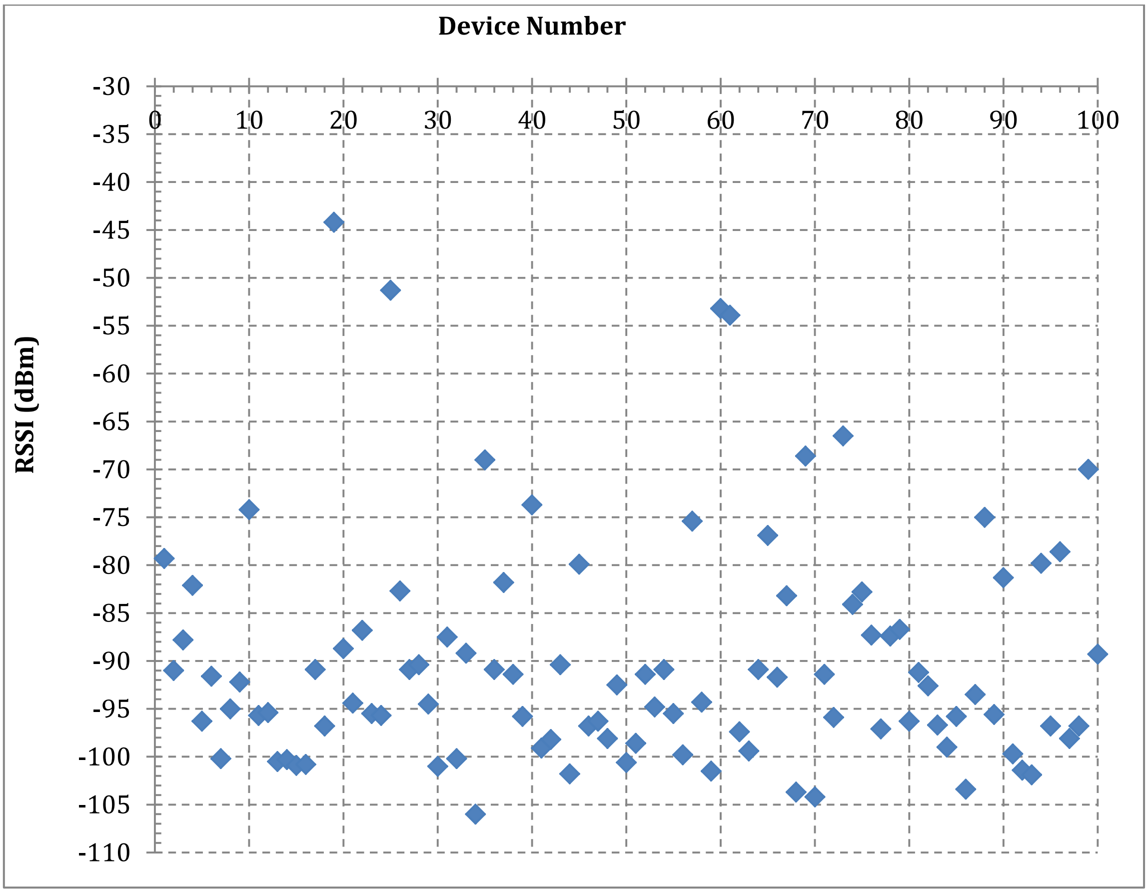

Figure 5; Figure 4; The scatter plot of computed RSSI for each sensor device.

Table 1 The detail values obtained for the 100 sensor devices x and y coordinates , distance, RSSI, hardware capacity

Device number	Hardware capacity	x-coordinate (m)	y-coordinate (m)	Distance (m) of the sensor devices from the LORAWAN Gateway	Pathloss (dB)	RSSI (dB)
1	3.9556	70.3503	499.005	503.94	75.2	-79.3
2	3.8518	804.727	111.191	812.372	83.8	-91.0
3	4.6749	50.0687	706.258	708.031	81.3	-87.8
4	3.1619	84.3057	555.691	562.049	77.2	-82.1
5	3.2952	615.547	821.22	1026.3	88.1	-96.3
6	2.798	114.141	825.868	833.718	84.3	-91.6
7	4.8496	965.415	753.466	1224.64	91.3	-100.2
8	4.1139	964.706	39.6525	965.52	87.0	-95.0
9	3.6987	852.479	81.1912	856.336	84.8	-92.2
10	4.0983	176.841	377.128	416.531	71.8	-74.2
11	3.8618	778.334	626.42	999.103	87.6	-95.7
12	4.1183	611.942	772.246	985.31	87.3	-95.4
13	3.8597	1148.11	480.991	1244.79	91.5	-100.5
14	4.3026	765.81	967.578	1233.97	91.4	-100.3
15	3.8062	944.39	847.664	1269.02	91.9	-100.9
16	4.9843	535.481	1143.01	1262.22	91.8	-100.8
17	3.0467	510.222	626.974	808.346	83.7	-90.9
18	2.7645	973.87	383.672	1046.72	88.4	-96.8
19	2.7742	98.4944	124.642	158.861	54.3	-44.2
20	2.659	157.142	720.931	737.859	82.1	-88.7
21	3.5114	204.599	918.987	941.487	86.5	-94.4
22	3.6209	461.307	499.674	680.058	80.6	-86.8
23	3.4145	981.028	107.171	986.865	87.4	-95.5
24	4.4088	947.97	314.436	998.758	87.6	-95.7
25	4.0697	71.356	181.315	194.851	58.0	-51.3
26	4.43	471.124	331.586	576.114	77.6	-82.7
27	4.8321	621.713	519.3	810.062	83.8	-90.9
28	4.9319	491.823	622.028	792.975	83.4	-90.4
29	2.9801	775.095	539.761	944.518	86.6	-94.5
30	2.8472	741.009	1032.94	1271.24	91.9	-101.0
31	4.2407	344.541	611.301	701.711	81.2	-87.5
32	2.7346	509.348	1113.47	1224.44	91.3	-100.2
33	3.8135	18.2748	752.497	752.719	82.5	-89.2
34	3.8259	1161.2	1130.08	1620.32	96.3	-106.0
35	4.6528	197.259	284.034	345.813	68.4	-69.0
36	3.7121	125.335	797.824	807.609	83.7	-90.9
37	3.4836	439.443	341.096	556.289	77.0	-81.8

38	4.1786	233.78	792.734	826.486	84.1	-91.4
39	4.3531	577.831	820.266	1003.36	87.7	-95.8
40	3.8001	400.602	80.2315	408.557	71.4	-73.7
41	3.3693	1122.92	300.652	1162.48	90.3	-99.1
42	2.875	1085.99	264.367	1117.71	89.6	-98.2
43	3.9652	62.1589	788.043	790.49	83.3	-90.4
44	3.1554	870.673	996.383	1323.2	92.7	-101.8
45	2.6111	317.561	406.466	515.809	75.6	-79.9
46	4.3873	498.946	921.013	1047.48	88.4	-96.8
47	3.107	646.488	796.892	1026.15	88.1	-96.3
48	3.606	1112.43	7.92405	1112.46	89.5	-98.1
49	4.2195	492.938	710.561	864.804	85.0	-92.5
50	3.3981	1160	456.39	1246.55	91.6	-100.6
51	4.3409	355.717	1080.87	1137.9	89.9	-98.6
52	3.4868	827.297	1.3583	827.298	84.2	-91.4
53	4.2085	786.28	545.69	957.086	86.8	-94.8
54	4.2601	636.169	500.732	809.595	83.8	-90.9
55	3.6058	823.764	543.881	987.114	87.4	-95.5
56	2.5489	786.503	908.788	1201.87	90.9	-99.8
57	3.3271	210.196	380.517	434.713	72.5	-75.4
58	3.5608	151.057	925.992	938.232	86.4	-94.3
59	3.1757	1178.91	556.201	1303.53	92.4	-101.5
60	2.9926	201.923	42.2	206.285	59.1	-53.2
61	4.5543	38.4689	207.532	211.067	59.5	-53.9
62	3.5748	662.216	851.674	1078.83	89.0	-97.4
63	4.7194	1040.6	558.713	1181.11	90.6	-99.4
64	3.478	789.627	180.211	809.93	83.8	-90.9
65	4.4228	224.711	402.527	461.002	73.6	-76.9
66	3.492	435.321	716.719	838.565	84.4	-91.7
67	4.5213	543.657	226.259	588.86	78.0	-83.2
68	4.3877	1158.33	871.344	1449.47	94.3	-103.7
69	3.4435	184.558	286.563	340.851	68.1	-68.6
70	3.04	1009.52	1082.56	1480.22	94.7	-104.2
71	4.476	760.822	317.493	824.41	84.1	-91.4
72	4.8733	444.001	903.29	1006.51	87.7	-95.9
73	3.3189	225.29	222.621	316.727	66.8	-66.5
74	4.1782	505.339	339.248	608.651	78.6	-84.1
75	3.5966	568.786	107.514	578.858	77.7	-82.8
76	4.5838	142.322	679.927	694.663	81.0	-87.3
77	4.4221	695.619	806.369	1064.95	88.7	-97.1
78	2.9181	266.901	644.98	698.023	81.1	-87.4

79	4.655	453.851	502.36	677.012	80.5	-86.7
80	4.9747	687.924	760.443	1025.43	88.0	-96.3
81	3.7861	297.131	764.189	819.922	84.0	-91.2
82	4.7107	342.72	801.24	871.46	85.1	-92.6
83	3.9701	728.167	750.228	1045.5	88.4	-96.7
84	2.8869	313.031	1115.31	1158.4	90.2	-99.0
85	2.9997	972.764	246.543	1003.52	87.7	-95.8
86	3.5174	1159.54	836.952	1430.05	94.1	-103.4
87	4.3718	861.694	278.752	905.659	85.8	-93.5
88	4.564	405.775	140.888	429.538	72.3	-75.0
89	4.4749	689.202	716.619	994.254	87.5	-95.6
90	3.2963	127.167	531.162	546.173	76.7	-81.3
91	3.8352	1069.44	541.296	1198.63	90.9	-99.7
92	2.7249	1037.99	781.095	1299.05	92.3	-101.4
93	2.7793	964.958	908.937	1325.64	92.7	-101.9
94	2.8407	307.659	413.257	515.204	75.6	-79.8
95	4.1966	701.34	781.171	1049.81	88.5	-96.8
96	3.7379	26.5649	491.067	491.785	74.8	-78.6
97	2.9743	501.806	993.476	1113.02	89.5	-98.1
98	3.7375	369.008	982.842	1049.83	88.5	-96.8
99	2.869	190.552	302.6	357.599	69.0	-70.0
100	2.6374	210.944	723.884	753.993	82.5	-89.3

III. RESULTS AND DISCUSSION

Hardware capacity (HWC) of 4.0 was selected as the threshold value for candidate cluster heads while the RSSI range of -75 dB ≤ RSSI ≤ -60 dB was selected for candidate cluster heads. That means , only sensor nodes with the hardware capacity greater than 4.0 (HWC > 4.0) and RSSI values in the range of -75 dB ≤ RSSI ≤ -60 dB can be selected by the SOM cluster algorithm as cluster heads. Based on the selected values of HWC and RSSI, the SOM algorithm was implemented in Matlab software for selecting the cluster heads from the 100 sensor nodes. The result of the SOM clustering is shown in Figure 6. Specifically, Figure 6 presents the SOM topology which shows that 16 cluster heads were selected from the 100 sensor nodes. The device number of each of the 16 cluster heads are also indicated in Figure 6 and Table 2. The results in Table 2, Figure 7 and Figure 8 also show the number of slave nodes that are clustered to each of the 16 cluster heads. According to the results in Table 2, Figure 7 , Figure 8 , Figure 9 and Figure 10, the 16th cluster head with RSSI of -63 dB and hardware capacity of 4.564 had the highest number of 9 slave sensor nodes whereas , the 2^{nd} cluster head with RSSI of -70.066dB and hardware capacity of 4.8496 and 3rd cluster heads with RSSI of -70.254dB and hardware capacity of 4.9843 had the lowest number of 3 slave sensor nodes.

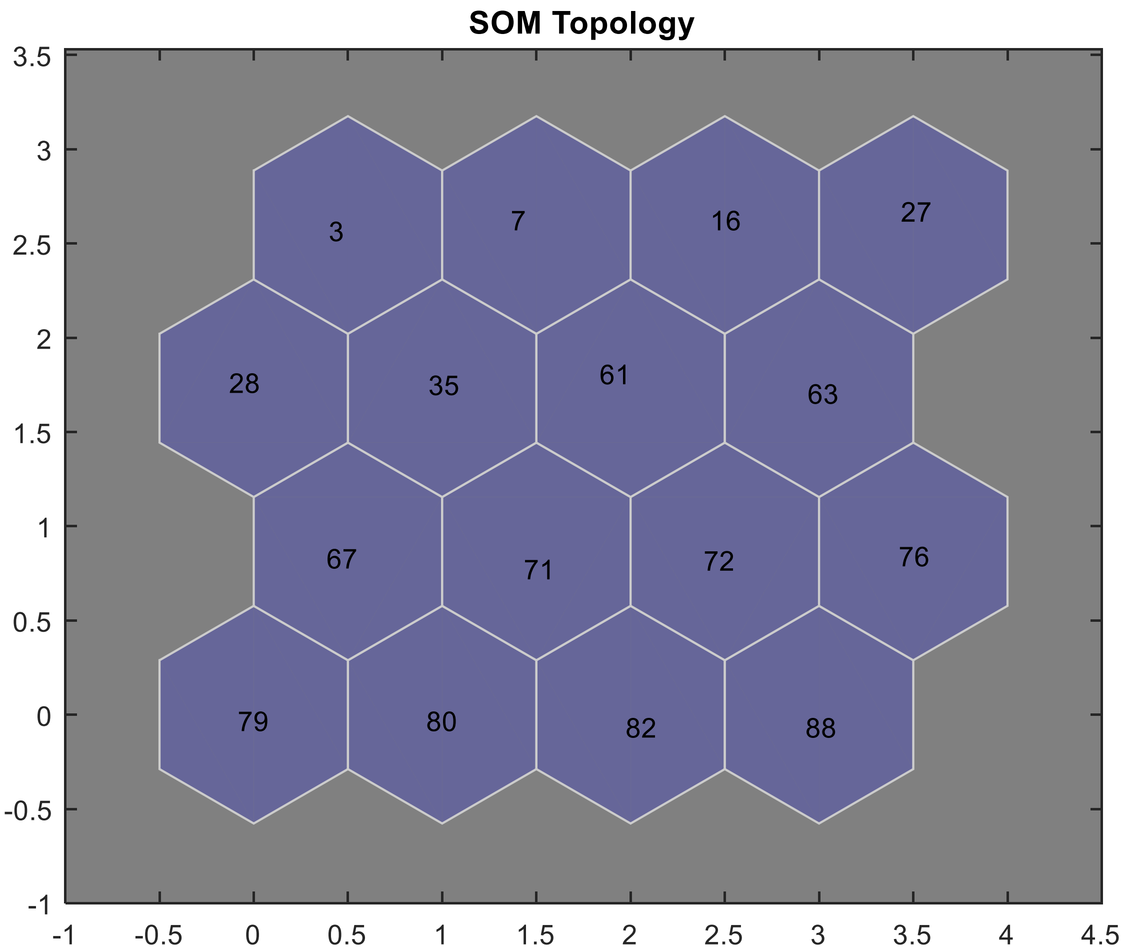

Figure 6; SOM topology showing the 16 cluster heads selected from the 100 sensor nodes.

Table ; SOM clustering results showing the list of selected cluster heads and the number of slave nodes that are clustered to each of the cluster head

Cluster heads number	Device Number Selected As The Cluster Head	x-coordinate of the Cluster Head	y-coordinate of the Cluster Head	Resultant distance of the Cluster Head	pathloss of the Cluster Head	RSSI of the Cluster Head	Hardware capacity of the Cluster Head	Number of slave nodes to the cluster head
1	3	42.431	598.52	600.03	146.83	-66.667	4.6749	8
2	7	818.15	638.53	1037.8	151.59	-70.066	4.8496	3
3	16	453.8	968.65	1069.7	151.86	-70.254	4.9843	3
4	27	526.88	440.09	686.49	148	-67.502	4.8321	4
5	28	416.8	527.14	672.01	147.82	-67.37	4.9319	7
6	35	167.17	240.71	293.06	140.61	-62.221	4.6528	7
7	61	32.601	175.87	178.87	136.32	-59.158	4.5543	5
8	63	881.87	473.49	1000.9	151.28	-69.842	4.7194	8
9	67	460.73	191.75	499.03	145.23	-65.524	4.5213	8
10	71	644.76	269.06	698.65	148.16	-67.611	4.476	7
11	72	376.27	765.5	852.98	149.89	-68.849	4.8733	5
12	76	120.61	576.21	588.7	146.67	-66.549	4.5838	6

13	79	384.62	425.73	573.74	146.44	-66.389	4.655	4
14	80	582.99	644.44	869.01	150.05	-68.965	4.9747	8
15	82	290.44	679.02	738.53	148.64	-67.956	4.7107	8
16	88	343.88	119.4	364.01	142.49	-63.566	4.564	9

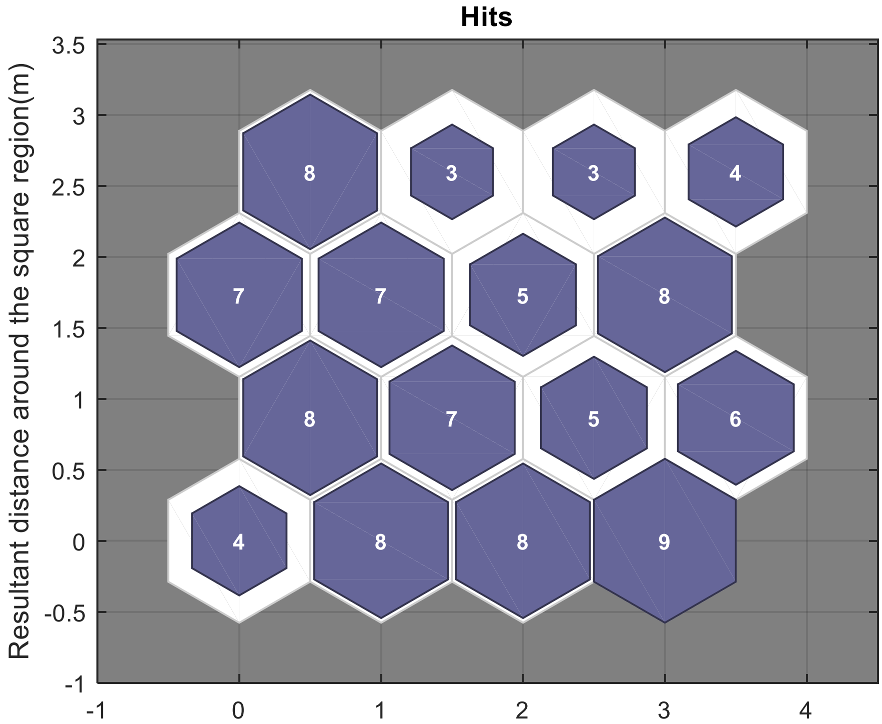

Figure 7; The SOM topology which the number of slave nodes that are clustered to each of the 16 cluster heads

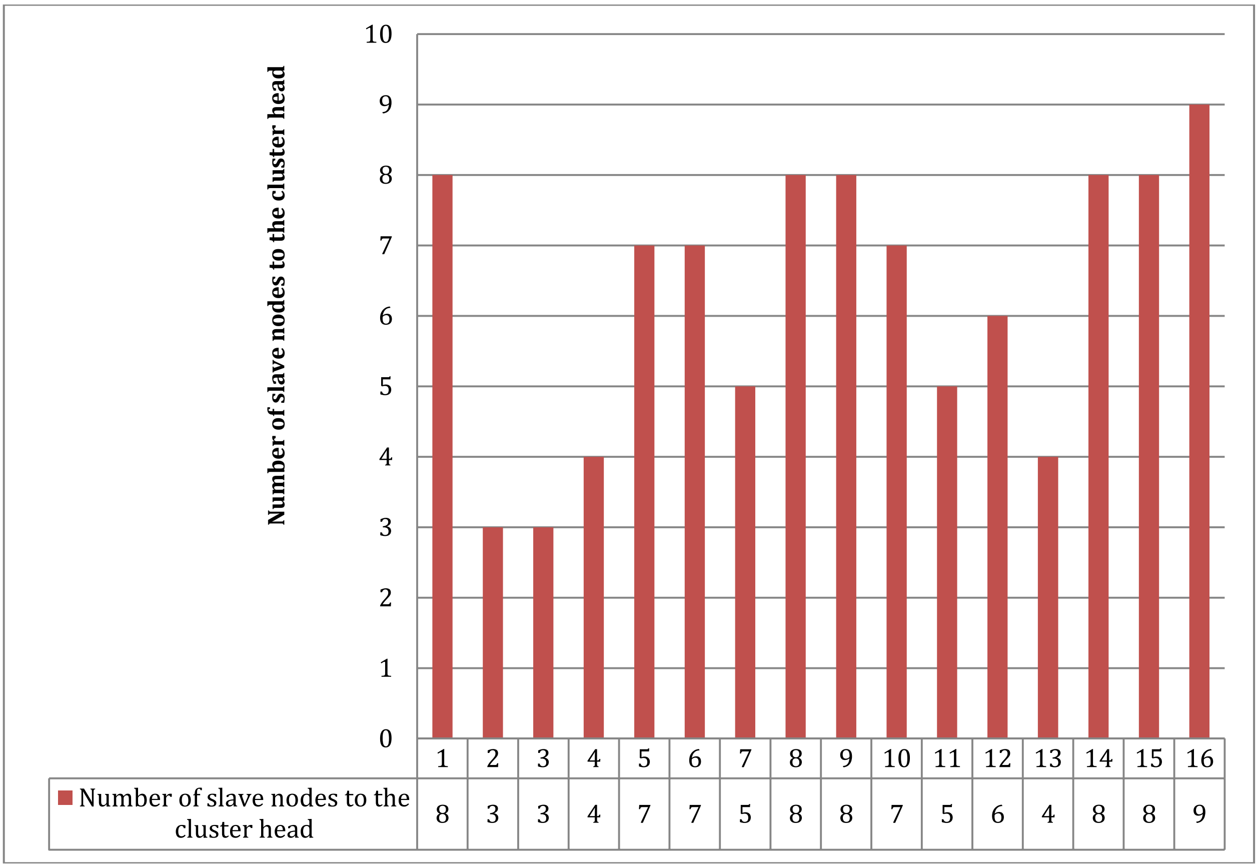

Figure 8; The Bar chart of the number of slave nodes that are clustered to each of the 16 cluster heads

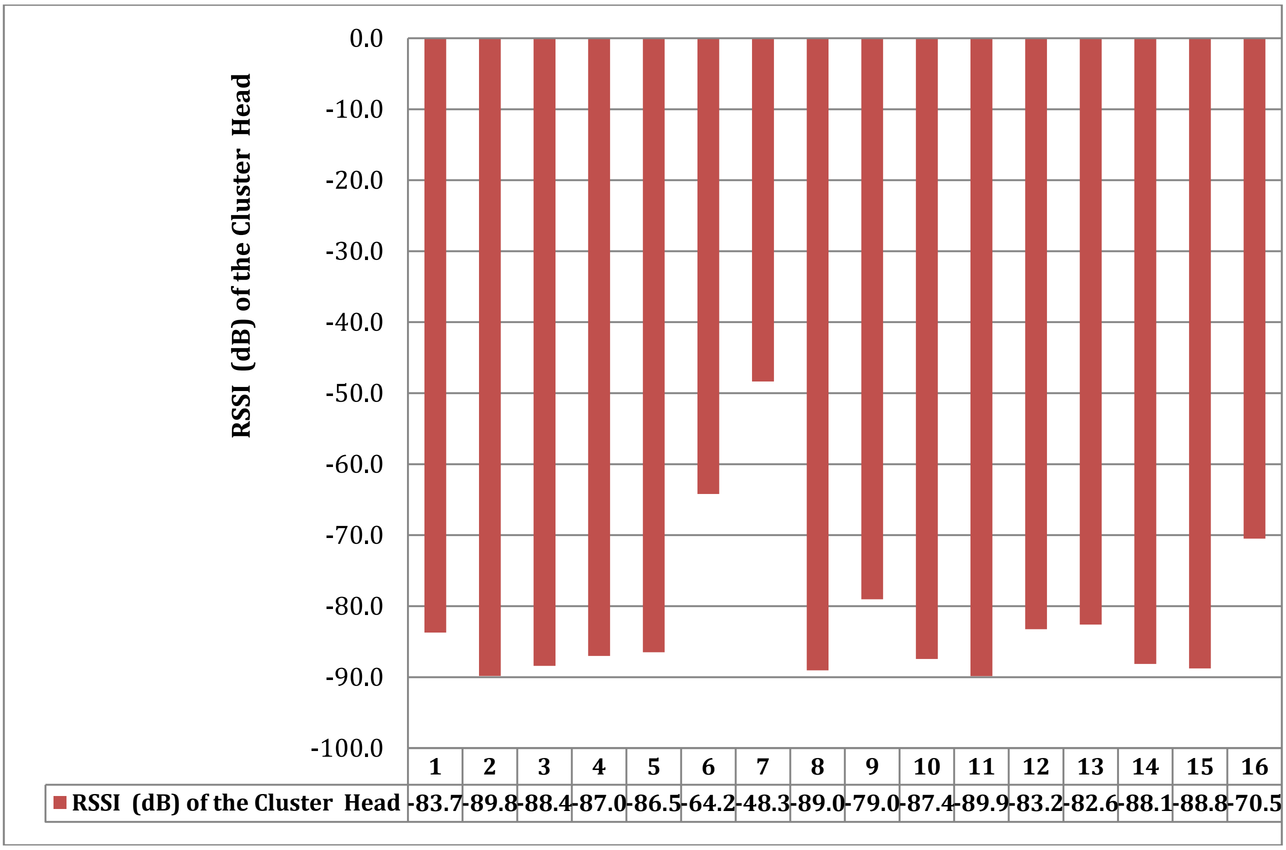

Figure 9; The Bar chart of the RSSI of each of the 16 cluster heads

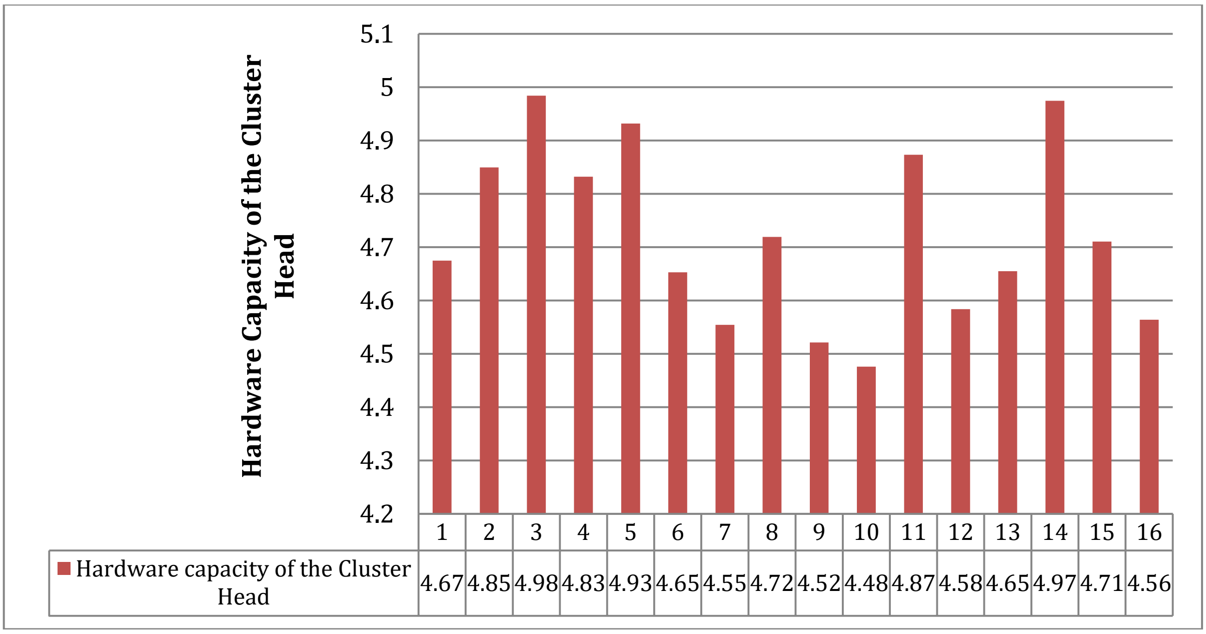

Figure 10; The Bar chart of the hardware capacity of each of the 16 cluster heads

IV. CONCLUSION

The Long Range Wide Area Network (LORAWAN) node clustering using self organizing map (SOM) algorithm is presented. The SOM algorithm utilized received signal strength intensity (RSSI) and the sensor device hardware capacity are the parameter for the selection of the cluster heads. The RSSI was determined based on Erceg pathloss model employed in link budget formula. In a set of 100 sensor nodes considered, only 16 cluster heads were selected based on the set threshold values for the hardware capacity and RSSI. In all, the results showed that the parameters used in the selection of cluster heads significantly affect the outcome of the SOM algorithm.

References

1) Eremia, Mircea, Lucian Toma, and Mihai Sanduleac. "The smart city concept in the 21st century." *Procedia Engineering* 181 (2017): 12-19.
2) Milošević, Mimica R., et al. "Smart city: Modeling key indicators in Serbia using IT2FS." *Sustainability* 11.13 (2019): 3536.
3) Trung, Truong Thanh. "Smart City and Modelling of Its Unorganized Flows Using Cell Machines." *Civil Engineering Journal* 6.5 (2020): 954-960.
4) Liu, Yan-Ting, et al. "A solar powered long range real-time water quality monitoring system by LoRaWAN." *2018 27th Wireless and Optical Communication Conference (WOCC)*. IEEE, 2018.
5) Muzammir, Muhammad Izzam, et al. "Performance analysis of LoRaWAN for indoor application." *2019 IEEE 9th Symposium on Computer Applications & Industrial Electronics (ISCAIE)*. IEEE, 2019.
6) Wu, Shiyang, et al. "Long range wide area network for agricultural wireless underground sensor networks." *Journal of Ambient Intelligence and Humanized Computing* (2020): 1-17.
7) Teizer, J., et al. "Construction resource efficiency improvement by Long Range Wide Area Network tracking and monitoring." *Automation in Construction* 116 (2020): 103245.
8) Kwasme, Hussein, and Sabit Ekin. "RSSI-based localization using LoRaWAN technology." *IEEE Access* 7 (2019): 99856-99866.
9) Marais, Jaco Morné, Adnan M. Abu-Mahfouz, and Gerhard P. Hancke. "A Survey on the Viability of Confirmed Traffic in a LoRaWAN." *IEEE Access* 8 (2020): 9296-9311.
10) Nanda, Ipseeta, and Sudha Chaudhary. "A Survey on Long Range Wide Area Network (LoRaWAN)." *Journal of Advanced Research in Networking and Communication Engineering* 2.2 (2019): 5-10.
11) Taha, Ashraf A., Mohamed F. Feteiha, and Wadood Abdul. "Performance evaluation for LoRa transceiver." *International Journal of Computer Science and Software Engineering* 8.2 (2019): 25-39.
12) Sahoo, Udaya Kumar, and Bijayananda Patnaik. "Design and implementation of remote monitoring system of solar lanterns, based on lorawan and cloud technology." *2017 International Conference on Computing Methodologies and Communication (ICCMC)*. IEEE, 2017.
13) Dalkic, Yurdaer, and Zoubida Alshekhly. "Development and design of a prototype for monitoring the water level in water wells using LoRaWAN." (2018).
14) Tehrani, Yas Hosseini, Ziba Fazel, and Seyed Mojtaba Atarodi. "A Survey of Two Dominant Low Power and Long Range Communication Technologies." *Information Systems & Telecommunication*: 60.
15) Galiulina, Irina, and Patrik Karlstén. "The suitability of LoRaWAN for battery powered security solutions." (2018).
16) Cardei, Mihaela, and Jie Wu. "Energy-efficient coverage problems in wireless ad-hoc sensor networks." *Computer communications* 29.4 (2006): 413-420.
17) Mostafaei, Habib. "Energy-efficient algorithm for reliable routing of wireless sensor networks." *IEEE Transactions on Industrial Electronics* 66.7 (2018): 5567-5575.
18) Boukerche, Azzedine, and Peng Sun. "Connectivity and coverage based protocols for wireless sensor networks." *Ad Hoc Networks* 80 (2018): 54-69.
19) Amutha, J., Sandeep Sharma, and Jaiprakash Nagar. "WSN strategies based on sensors, deployment, sensing models, coverage and energy efficiency: Review, approaches and open issues." *Wireless Personal Communications* 111.2 (2020): 1089-1115.
20) Liew, Soung-Yue, et al. "A fast, adaptive, and energy-efficient data collection protocol in multi-channel-multi-path wireless sensor networks." *IEEE Computational Intelligence Magazine* 13.1 (2018): 30-40.
21) Akila, I. S., S. V. Manisekaran, and S. V. Venkatesan. "Modern Clustering Techniques in Wireless Sensor Networks." *Wireless Sensor Networks—Insights and Innovations; Sallis, PJ; Ed.; InTech Open: London, UK* (2017): 141-156.
22) Warrier, Maya M., and Ajay Kumar. "An energy efficient approach for routing in wireless sensor networks." *Procedia Technology* 25 (2016): 520-527.
23) Sinde, Ramadhani, et al. "Refining Network Lifetime of Wireless Sensor Network Using Energy-Efficient Clustering and DRL-Based Sleep Scheduling." *Sensors* 20.5 (2020): 1540.

24) Behera, Trupti Mayee, et al. "Residual energy-based cluster-head selection in WSNs for IoT application." *IEEE Internet of Things Journal* 6.3 (2019): 5132-5139.
25) Chattopadhyay, Manojit, Pranab K. Dan, and Sitanath Mazumdar. "Application of visual clustering properties of self organizing map in machine–part cell formation." *Applied soft computing* 12.2 (2012): 600-610.
26) Chaudhary, Vikas, R. S. Bhatia, and Anil K. Ahlawat. "A novel Self-Organizing Map (SOM) learning algorithm with nearest and farthest neurons." *Alexandria Engineering Journal* 53.4 (2014): 827-831.
27) Yang, Le, Zhongbin Ouyang, and Yong Shi. "A modified clustering method based on self-organizing maps and its applications." *Procedia Computer Science* 9 (2012): 1371-1379.
28) Ilc, Nejc, and Andrej Dobnikar. "Gravitational clustering of the self-organizing map." *International Conference on Adaptive and Natural Computing Algorithms*. Springer, Berlin, Heidelberg, 2011.
29) Miljković, Dubravko. "Brief review of self-organizing maps." *2017 40th International Convention on Information and Communication Technology, Electronics and Microelectronics (MIPRO)*. IEEE, 2017.
30) Vesanto, Juha, and Esa Alhoniemi. "Clustering of the self-organizing map." *IEEE Transactions on neural networks* 11.3 (2000): 586-600.
31) Mason, Samuel P. *Atmospheric effects on radio frequency (RF) wave propagation in a humid, near-surface environment*. Naval Postgraduate School Monterey Ca, 2010.
32) Tang, Weisheng, et al. "Measurement and Analysis of Near-Ground Propagation Models under Different Terrains for Wireless Sensor Networks." *Sensors* 19.8 (2019): 1901.
33) Souza Bezerra,Níbia, et al. "Temperature Impact in LoRaWAN—A Case Study in Northern Sweden." *Sensors* 19.20 (2019): 4414.
34) Halifa, Awal, Eric Tutu Tchao, and Jerry John Kponyo. "Investigating the best radio propagation model for 4G-WiMAX networks deployment in 2530MHz Band in Sub-Saharan Africa." *arXiv preprint arXiv:1711.08065* (2017).
35) Luomala, Jari, and Ismo Hakala. "Effects of temperature and humidity on radio signal strength in outdoor wireless sensor networks." *2015 Federated Conference on Computer Science and Information Systems (FedCSIS)*. IEEE, 2015.
36) Chimaobi, Nnadi Nathaniel, Charles Chukwuemeka Nnadi, and Amaechi Justice Nzegwu. "Comparative Study of Least Square Methods for Tuning Erceg Pathloss Model." *American Journal of Software Engineering and Applications* 6.3 (2017): 61-66.
37) Jain, Raj. "Channel models: A tutorial." *WiMAX forum AATG*. Vol. 10. Washington Univ. St. Louis, Dept. CSE, 2007.
38) Joseph, Wout, Laurens Roelens, and Luc Martens. "Path loss model for wireless applications at 3500 MHz." *2006 IEEE Antennas and Propagation Society International Symposium*. IEEE, 2006.
39) Cardei, Mihaela, and Jie Wu. "Energy-efficient coverage problems in wireless ad-hoc sensor networks." *Computer communications* 29.4 (2006): 413-420.